Cellular Microbiology (2017) **19**(1), e12619
doi:10.1111/cmi.12619
First published online 11 July 2016

LppM impact on the colonization of macrophages by *Mycobacterium tuberculosis*

Nathalie Deboosère,[1,2,3,4,5] Raffaella Iantomasi,[1,2,3,4,5,†] Christophe J. Queval,[1,2,3,4,5,†] Ok-Ryul Song,[1,2,3,4,5,†] Gaspard Deloison,[1,2,3,4,5] Samuel Jouny,[1,2,3,4,5] Anne-Sophie Debrie,[1,2,3,4,5] Mathias Chamaillard,[1,2,3,4,5] Jérôme Nigou,[6] Martin Cohen-Gonsaud,[7] Camille Locht,[1,2,3,4,5] Priscille Brodin[1,2,3,4,5*] and Romain Veyron-Churlet[1,2,3,4,5*]

[1]*Univ. Lille, U1019 – UMR 8204 – CIIL – Centre d'Infection et d'Immunité de Lille, Lille F-59000, France.*
[2]*CNRS, UMR 8204, Lille F-59000, France.*
[3]*Inserm U1019, Lille F-59000, France.*
[4]*CHU Lille, Lille F-59000, France.*
[5]*Institut Pasteur de Lille, Lille F-59000, France.*
[6]*Institut de Pharmacologie et de Biologie Structurale, Université de Toulouse CNRS, Toulouse F-31077, France.*
[7]*Centre de Biochimie Structurale, CNRS UMR 5048, Inserm U1054, Université de Montpellier, Montpellier F-34090, France.*

Summary

Mycobacterium tuberculosis **produces several bacterial effectors impacting the colonization of phagocytes. Here, we report that the putative lipoprotein LppM hinders phagocytosis by macrophages in a toll-like receptor 2-dependent manner. Moreover, recombinant LppM is able to functionally complement the phenotype of the mutant, when exogenously added during macrophage infection. LppM is also implicated in the phagosomal maturation, as a lppM deletion mutant is more easily addressed towards the acidified compartments of the macrophage than its isogenic parental strain. In addition, this mutant was affected in its ability to induce the secretion of pro-inflammatory chemokines, interferon-gamma-inducible protein-10, monocyte chemoattractant protein-1 and macrophage inflammatory protein-1α. Thus, our results describe a new mycobacterial protein involved in the early trafficking of the tubercle bacillus and its manipulation of the host immune response.**

Received 25 August, 2015; revised 10 May, 2016; accepted 12 May, 2016. *For correspondence. E-mails priscille.brodin@inserm.fr (P. Brodin); romain_veyron@yahoo.fr (R. Veyron-Churlet); Tel. + 33 320 87 11 84; Fax + 33 320 87 11 92
†Equal contribution of the second authors.

Introduction

Tuberculosis (TB) remains a leading infectious disease around the world with 1.5 million deaths and 9.6 million new cases per year. Approximately one-third of the world population is considered to have latent TB, and although they show no clinical symptoms, they are at risk to progress to active disease (Barry *et al.*, 2009; Young *et al.*, 2009). The treatment of active TB requires chemotherapy to be taken for at least 6 months, which often leads to a poor compliance because of the toxicity of the treatment and thereby to the emergence of multi-drug-resistant or extremely-drug-resistant strains of *Mycobacterium tuberculosis*. The emergence of totally drug-resistant strains of *M. tuberculosis* has become a major global threat (Klopper *et al.*, 2013), urging the need to better understand TB pathogenesis in order to develop new and more potent drugs. TB pathogenesis is linked to a tight interplay between the host immune response and *M. tuberculosis*, which produces factors that contribute to its successful colonization and its persistence within host cells. Tubercle bacilli are able to infect macrophages and to actively replicate within their phagosomes. After interaction with several cell-host receptors and subsequent phagocytosis, the bacilli are able to block phagosomal maturation, to escape from the phagosome and to subvert the host immune response (for reviews (Killick *et al.*, 2013; Stanley and Cox, 2013)).

The cell colonization and intracellular trafficking of *M. tuberculosis* involve several distinct bacterial effectors, and deciphering the contribution of each of the different actors at the host-pathogen interface is essential to understand the intracellular persistence of *M. tuberculosis*. The bacterial virulence factors that have been extensively studied to impact on the invasion process are the ESX type VII secretion system, the serine protein kinase PknG, the lipid phosphatase SapM and components of the mycobacterial cell wall (Walburger *et al.*, 2004; Vergne *et al.*, 2005; Brodin *et al.*, 2006; Cambier *et al.*, 2014). Using a non-biased global screening approach on an 11 000 *M. tuberculosis* transposon mutant library, we identified additional mycobacterial genes whose expression impairment impacts the intracellular trafficking (Brodin *et al.*, 2010). Among these genes, *rv2171* (*lppM*) was shown to affect colocalization of *M. tuberculosis* Beijing GC1237 with LysoTracker, a marker of the acidic lysosomal compartment, suggesting that LppM is involved in preventing early phagosomal maturation in infected macrophages (Brodin *et al.*, 2010).

Interestingly, *lppM* expression has been shown to be induced during macrophage infection (Dubnau *et al.*, 2002), and it was recently selected by bioinformatic analysis as a potential *M. tuberculosis* effector involved in host–pathogen interaction (Li *et al.*, 2015).

In this study, we demonstrate that LppM limits the early step of *M. tuberculosis* entry into the macrophage. This phenotype can be reversed by the exogenous addition of recombinant LppM and is dependent on toll-like receptor 2 (TLR2). We further characterized the involvement of *lppM* in *M. tuberculosis* macrophage colonization by showing its implication in the blocking of the phagosomal maturation using different cellular markers: LysoTracker, lysosomal-associated membrane protein-1 (LAMP-1) and cathepsin D. Furthermore, we show that the *lppM* deletion mutant is affected in its ability to induce the secretion of the pro-inflammatory chemokines interferon-gamma-inducible protein-10 (IP-10) (CXCL10), monocyte chemoattractant protein-1 (MCP-1) (CCL2) and macrophage inflammatory protein-1α (MIP-1α) (CCL3). Altogether, these data suggest that LppM is an additional bacterial effector implicated in the early steps of *M. tuberculosis* infection.

Results

LppM hinders mycobacterial uptake into macrophages

To investigate the contribution of LppM in the colonization of macrophages, a *lppM* deletion mutant (*Mtb*H37RvΔ*lppM*) was constructed in *M. tuberculosis* H37Rv by substituting the *lppM* gene with a cassette coding for hygromycin resistance (Fig. S1A). Allelic exchange was confirmed by polymerase chain reaction (PCR) with the amplification of a 2.9 kb fragment (Fig. S1B) and checked by sequencing to confirm the insertion of the hygromycin-resistance cassette at the expected locus (data not shown). In axenic cultures of *M. tuberculosis* H37Rv, LppM is constitutively expressed, and its apparent migration weight around 28 kDa after SDS-PAGE is above its predicted molecular weight (Fig. S1C). As expected, the production of LppM was totally abolished in *M. tuberculosis* H37RvΔ*lppM* (Fig. S1C). The deletion mutant was complemented with a copy of *lppM* under the control of its own promoter (prom$_{lppM}$::*lppM*) or the strong *hsp60* promoter (prom$_{hsp60}$::*lppM*) in the integrative vector pMV306 (Fig. S1D).

DsRed-expressing *M. tuberculosis* H37Rv and *M. tuberculosis* H37RvΔ*lppM* were used to infect murine bone marrow-derived macrophages (BMDM) at multiplicities of infection (MOI) of 5 and 10, and uptake of fluorescent mycobacteria was determined 2 h post-infection. The percentage of BMDM containing bacteria was largely increased for *M. tuberculosis* H37RvΔ*lppM* in comparison with *M. tuberculosis* H37Rv (Fig. 1A). As the use of a third antibiotic marker was detrimental to the normal growth of *M. tuberculosis* H37RvΔ*lppM*, preventing complementation by an additional plasmid, we checked complementation by covalently staining the bacteria with the red fluorescent dye CypHer5E. Although labelling and detection were not as strong as DsRed-labelled bacteria, complementation of CypHer5E-labelled *M. tuberculosis* H37RvΔ*lppM* with prom$_{lppM}$::*lppM* vector restored the infectivity to levels similar to those of *M. tuberculosis* H37Rv (Fig. 1B). To discard any impact of clumping bacteria, we assessed the median of the bacterial area in infected BMDM. In these conditions, there was no difference between *M. tuberculosis* H37Rv and *M. tuberculosis* H37RvΔ*lppM*, indicating that the deletion of *lppM* did not increase clumping of the culture (Fig. S2A). On the contrary, heat-killed *M. tuberculosis* H37Rv and *M. tuberculosis* H37RvΔ*lppM* displayed a significantly higher bacterial area reflecting their tendency to form bigger aggregates (Fig. S2A).

To obtain insight into the fate of *M. tuberculosis* H37RvΔ*lppM* after macrophage uptake, we assessed the bacterial area at different time points (from Days 0 to 4) after BMDM infection, using a lower MOI of 2. As *M. tuberculosis* H37RvΔ*lppM* uptake was higher in comparison with *M. tuberculosis* H37Rv, each bacterial area was standardized by the corresponding bacterial area obtained at Day 0. In these conditions, *M. tuberculosis* H37RvΔ*lppM* growth in the macrophage was slower than that of *M. tuberculosis* H37Rv during the first 3 days of infection. However, *M. tuberculosis* H37RvΔ*lppM* growth was identical to that of the wild-type at Day 4 (Fig. S2B). These data illustrate the importance of LppM for the early steps of macrophage colonization and less so at later time points.

LppM hinders phagosomal maturation

To determine whether *M. tuberculosis* H37RvΔ*lppM* is affected in a subsequent early trafficking process, we investigated the effect of the *lppM* deletion on phagosome maturation. DsRed-labelled *M. tuberculosis* H37Rv-infected or *M. tuberculosis* H37RvΔ*lppM*-infected BMDM were stained with LysoTracker, a fluorescent marker of acidified cellular compartments and analysed by confocal imaging using a dedicated multiparameter automated image analysis system (Brodin *et al.*, 2010). This analysis showed that the percentage of bacteria colocalizing with LysoTracker was higher for *M. tuberculosis* H37RvΔ*lppM* than for *M. tuberculosis* H37Rv, indicating increased targeting of the mutant to the acidified compartment (Fig. 1C and D). The percentage of LysoTracker-positive cells was higher for *M. tuberculosis* H37RvΔ*lppM* than for *M. tuberculosis* H37Rv (Fig. S2C), in agreement with our previous observation on a Δ*lppM* transposon mutant in the *M. tuberculosis* Beijing GC1237 background (Brodin *et al.*, 2010). Complementation by *lppM* under the dependence of its own promoter restored the wild-type phenotype (Fig. S2C). However, as CypHer5E-staining is pH sensitive, we used DsRed-expressing bacteria to standardize the LysoTracker intensity to quantify the

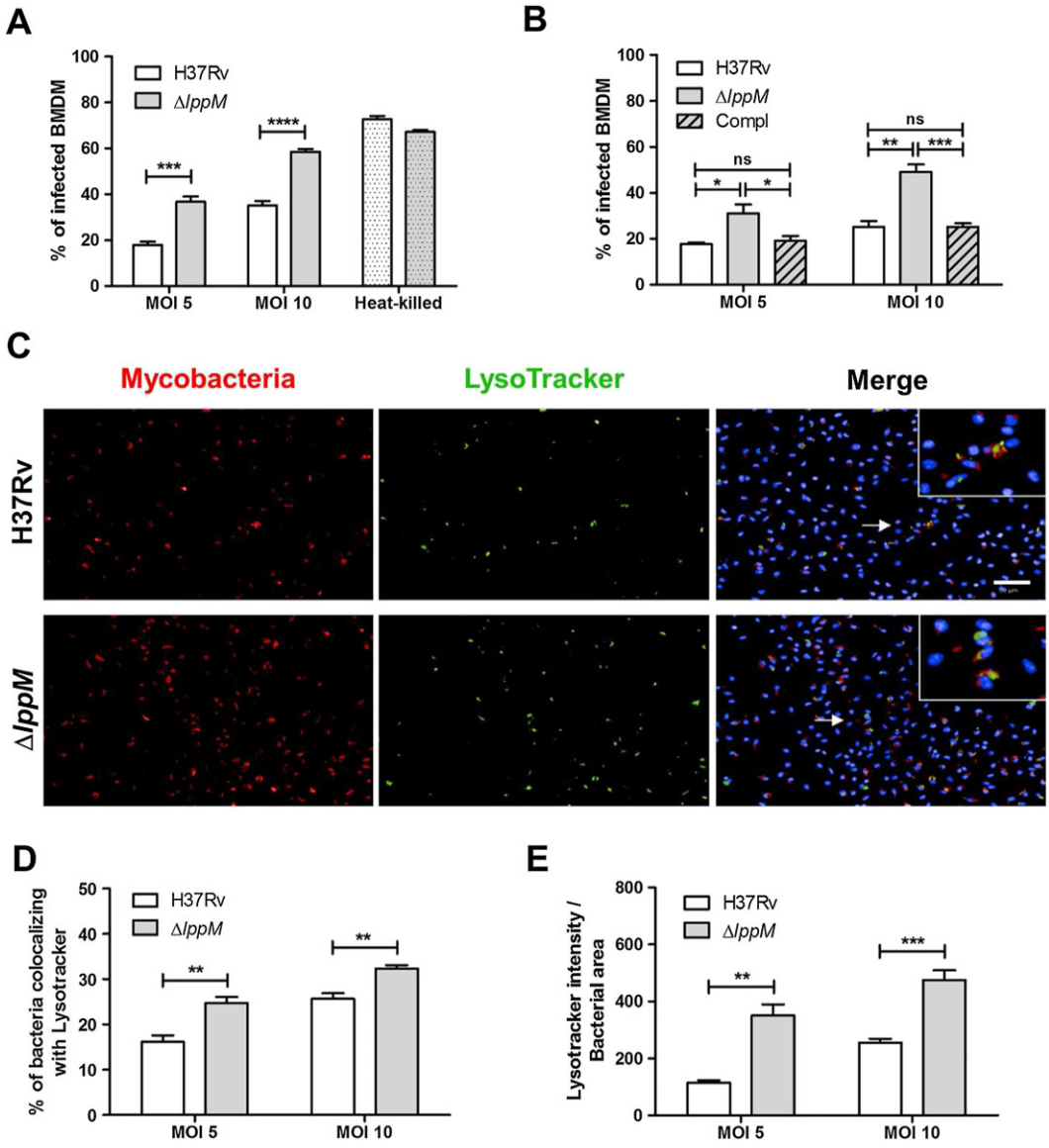

Fig. 1. *Mycobacterium tuberculosis* H37RvΔ*lppM* is more prone to phagocytosis by macrophages than *M. tuberculosis* H37Rv and is impaired in blocking phagosomal maturation.
A. Percentage of infected BMDM 2 h post-infection, using *M. tuberculosis* H37Rv or *M. tuberculosis* H37RvΔ*lppM* producing fluorescent DsRed, or their respective heat-killed bacteria [multiplicities of infection (MOI) 10] as a control.
B. Percentage of infected bone marrow-derived macrophages (BMDM) 2 h post-infection, using *M. tuberculosis* H37Rv, *M. tuberculosis* H37RvΔ*lppM* or the complemented strain (prom$_{lppM}$::*lppM*) labelled with CypHer5E.
C. DsRed-producing bacteria (red), LysoTracker staining (green) and Hoechst staining (blue) of BMDM infected with *M. tuberculosis* H37Rv or *M. tuberculosis* H37RvΔ*lppM*. The bar corresponds to 50 μm. Zoomed-in inset (right panel) corresponds to the area indicated by the white arrow.
D. Percentage of *M. tuberculosis* H37Rv or *M. tuberculosis* H37RvΔ*lppM* colocalizing with LysoTracker staining in BMDM.
E. Standardization of LysoTracker intensity by bacterial area among the population of *M. tuberculosis* H37Rv-infected or *M. tuberculosis* H37RvΔ*lppM*-infected BMDM. All graphs are representative of at least three independent experiments.

bacteria (bacterial area) present in the macrophages. This ratio highlights the increase of Lysotracker intensity in the case of *M. tuberculosis* H37RvΔ*lppM* compared with *M. tuberculosis* H37Rv, regardless of the number of intracellular bacteria, which reflects an enhanced acidification of the vacuoles containing *M. tuberculosis* H37RvΔ*lppM* (Fig. 1E). These results indicate that *lppM* partly contributes to the blocking of the phagosomal maturation by the bacilli.

This was further characterized by using other cellular markers: the LAMP-1 and the endosomal protease,

cathepsin D. Similarly to LysoTracker staining, LAMP-1 and cathepsin D colocalized at a significantly higher extent with *M. tuberculosis* H37RvΔ*lppM* compared with *M. tuberculosis* H37Rv (Fig. 2A–D), confirming the role of LppM in the early steps of macrophage infection.

Recombinant ^{6}His-LppM$_{26–185}$ limits phagocytosis

Recombinant soluble ^{6}His-LppM$_{26–185}$, starting right after the residue Cys$_{25}$ and devoid of the putative C-terminal transmembrane domain (Barthe *et al.*, unpublished), was produced in *Escherichia coli* (Fig. 3A). When ^{6}His-LppM$_{26–185}$

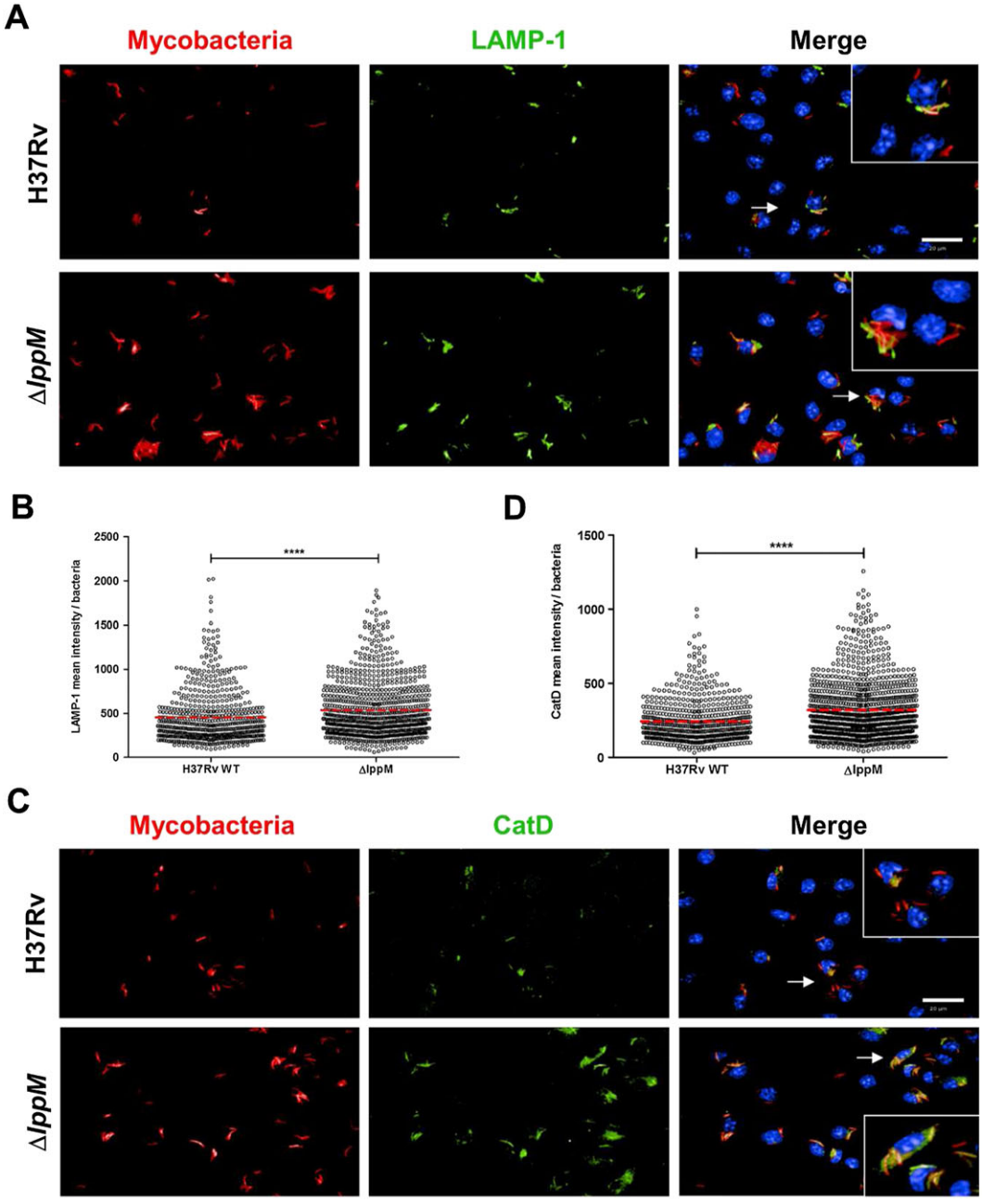

Fig. 2. *Mycobacterium tuberculosis* H37RvΔ*lppM* is more easily addressed towards the degradative compartments of macrophages than *M. tuberculosis* H37Rv.

A. DsRed-producing bacteria (red), lysosomal-associated membrane protein-1 (LAMP-1) staining (green) and Hoechst staining (blue) of bone marrow-derived macrophages (BMDM) infected with *M. tuberculosis* H37Rv or *M. tuberculosis* H37RvΔ*lppM*. The bar corresponds to 20 μm. Zoomed-in inset (right panel) corresponds to the area indicated by the white arrow.

B. LAMP-1 mean intensity per bacteria after infection of BMDM with *M. tuberculosis* H37Rv or *M. tuberculosis* H37RvΔ*lppM*.

C. DsRed-producing bacteria (red), Cathepsin D (CatD) staining (green) and Hoechst staining (blue) of BMDM infected with *M. tuberculosis* H37Rv or *M. tuberculosis* H37RvΔ*lppM*. The bar corresponds to 20 μm. Zoomed-in inset (right panel) corresponds to the area indicated by the white arrow.

D. Cathepsin D mean intensity per bacteria after infection of BMDM with *M. tuberculosis* H37Rv or *M. tuberculosis* H37RvΔ*lppM*.

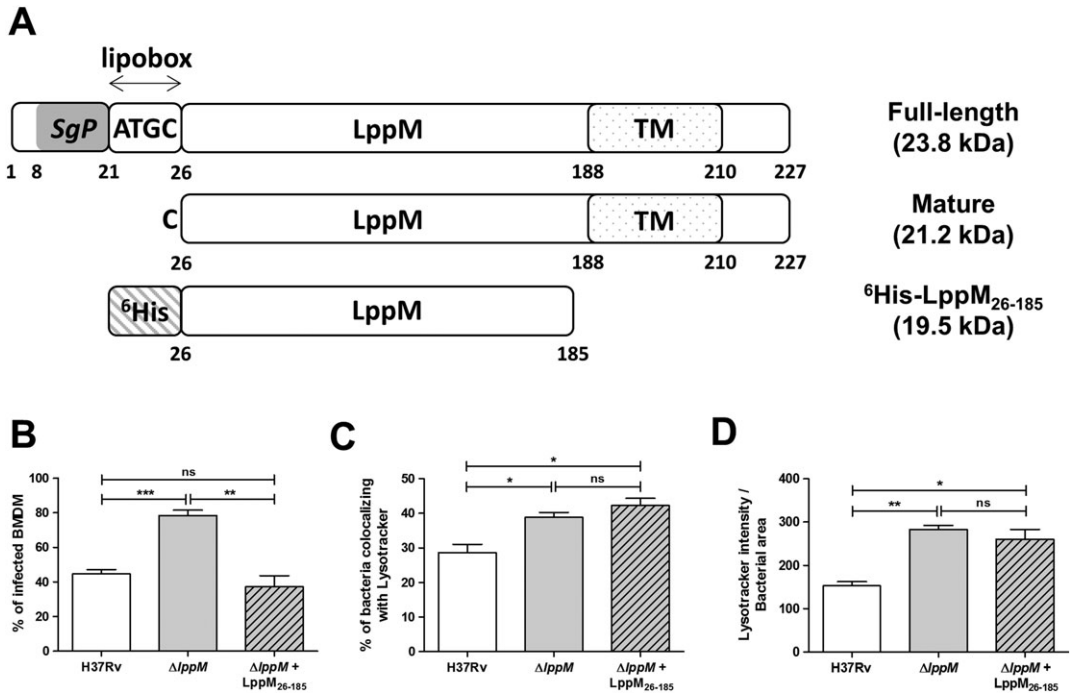

Fig. 3. LppM impacts phagocytosis by bone marrow-derived macrophages (BMDM).
A. Schematic representation of the different forms of LppM with their molecular weight. The "full-length" LppM corresponds to the entire protein containing a signal peptide (SgP, grey box), a putative lipobox motif ($_{22}$ATGC$_{25}$) and a transmembrane sssdomain (TM, dotted box). The mature LppM corresponds to the form after cleavage of its signal peptide, starting at Cys$_{25}$. Soluble domain of LppM corresponds to the N-terminal ^{6}His-tagged (stripped box) construction lacking the initial cysteine (Cys$_{25}$) and its C-terminal transmembrane domain.
B. Complementation of the *Mycobacterium tuberculosis* H37Rv*ΔlppM* phagocytosis phenotype by adding 10 μM of the recombinant LppM (^{6}His-LppM$_{26–185}$) purified from *Escherichia coli*.
C. Percentage of *M. tuberculosis* H37Rv and *M. tuberculosis* H37Rv*ΔlppM*, without or with addition of ^{6}His-LppM$_{26–185}$, colocalizing with LysoTracker staining in BMDM.
D. Standardization of LysoTracker intensity by bacterial area among the population of *M. tuberculosis* H37Rv-infected and *M. tuberculosis* H37Rv*ΔlppM*-infected BMDM, without or with addition of ^{6}His-LppM$_{26–185}$. All graphs are representative of at least two independent experiments.

was added to the medium of *M. tuberculosis* H37Rv*ΔlppM*, the phagocytosis level of the mutant strain was reduced to that of *M. tuberculosis* H37Rv (Fig. 3B). This complementation of the uptake defect did not depend on LppM acylation, as Cys$_{25}$ was not present in ^{6}His-LppM$_{26–185}$, inferring that LppM action is mediated by another structural element. However, the addition of ^{6}His-LppM$_{26–185}$ did not complement the *M. tuberculosis* H37Rv*ΔlppM* phenotype regarding the bacterial colocalization with acidified compartments (Fig. 3C) or LysoTracker intensity (Fig. 3D).

Phenotype of Mycobacterium tuberculosis *H37RvΔlppM is mediated by toll-like receptor 2-dependent signalling*

Toll-like receptor 2 operates as a primary sensor of a large variety of mycobacterial components and thereby triggers innate immune responses (Underhill *et al*., 1999; Harding and Boom, 2010). Therefore, we examined the effect of the *lppM* deletion on murine TLR2$^{-/-}$ BMDM. Interestingly, no difference was observed between *M. tuberculosis* H37Rv and *M. tuberculosis* H37Rv*ΔlppM* in bacterial uptake by TLR2$^{-/-}$ BMDM (Fig. 4A). Bacterial colocalization in the acidified compartments of TLR2$^{-/-}$ BMDM was also similar between *M. tuberculosis* H37Rv and *M. tuberculosis* H37Rv*ΔlppM* (Fig. 4B and C). In addition, there was no significant difference in Lysotracker intensity when TLR2$^{-/-}$ BMDM were infected with *M. tuberculosis* H37Rv or *M. tuberculosis* H37Rv*ΔlppM* (Fig. 4D). These results indicate that LppM modulates bacterial uptake through TLR2 signalling.

Mycobacterium tuberculosis *H37RvΔlppM induces reduced secretion of pro-inflammatory chemokines over* Mycobacterium tuberculosis *H37Rv*

We used the Luminex technology to further characterize the cytokine signatures induced by *M. tuberculosis* H37Rv*ΔlppM*. *M. tuberculosis* H37Rv*ΔlppM* was affected in its ability to induce the secretion of the pro-inflammatory chemokines IP-10 (Fig. 5A), MCP-1 (Fig. 5B) and MIP-1α (Fig. 5C), and this phenotype was (partially) reversed with the complemented strain. In contrast to the phagocytosis phenotype, the defect in chemokine secretion was not mediated by TLR2, as the profile of chemokines was almost identical between wild-type and TLR2$^{-/-}$ BMDM infected by *M. tuberculosis* H37Rv*ΔlppM* (Fig. 5A–C). As LppM is

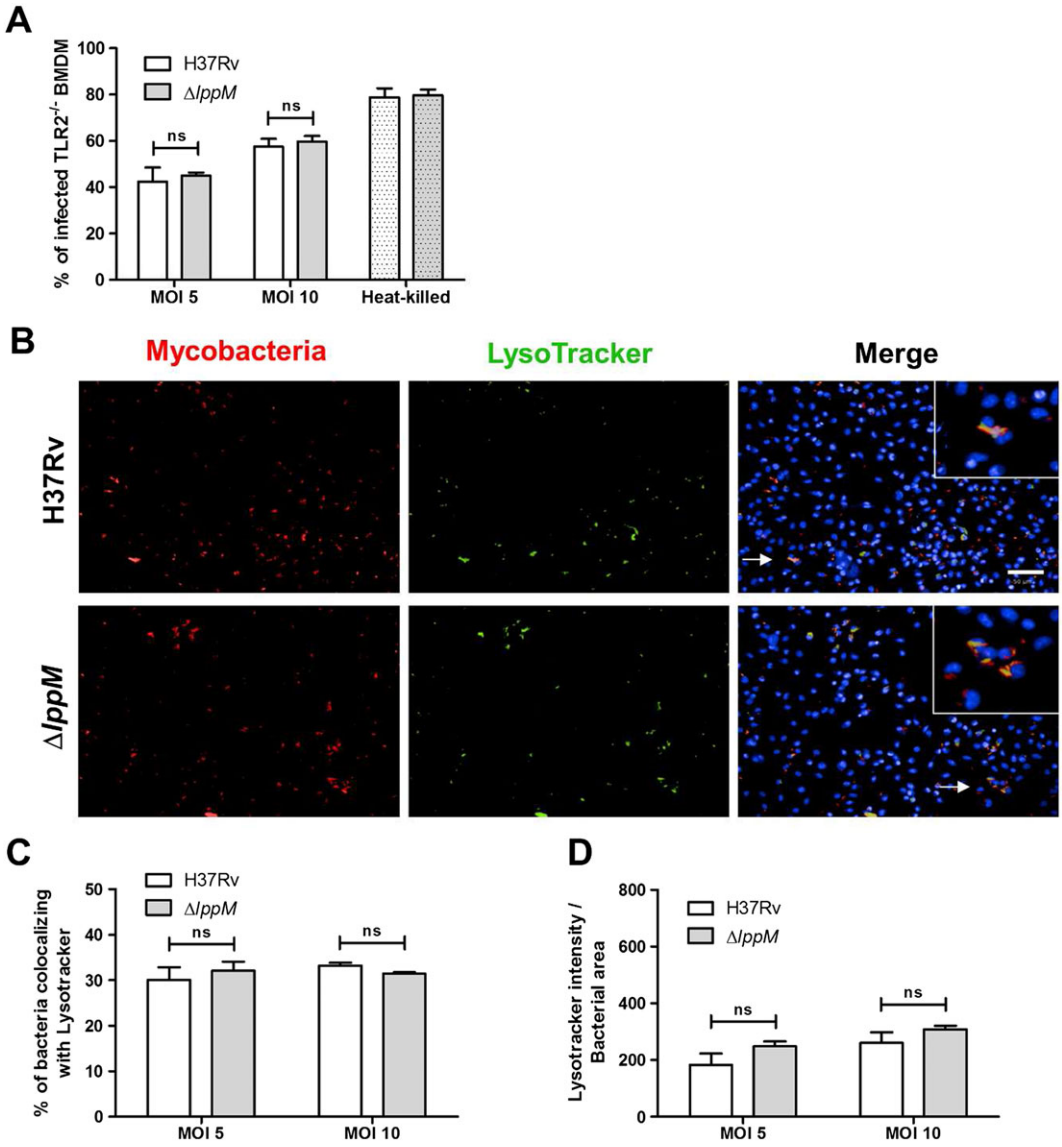

Fig. 4. *Mycobacterium tuberculosis* H37RvΔ*lppM* mutant phenotype depends on toll-like receptor 2 (TLR2)-signalling.
A. Percentage of infected TLR2$^{-/-}$ BMDM 2 h post-infection, using *M. tuberculosis* H37Rv or *M. tuberculosis* H37RvΔ*lppM* producing DsRed and respective heat-killed bacteria [multiplicities of infection (MOI) 10] as a control.
B. DsRed-producing bacteria (red), LysoTracker staining (green) and Hoechst staining (blue) of TLR2$^{-/-}$ BMDM infected with *M. tuberculosis* H37Rv or *M. tuberculosis* H37RvΔ*lppM*. The bar corresponds to 50 μm.
C. Percentage of *M. tuberculosis* H37Rv or *M. tuberculosis* H37RvΔ*lppM* colocalizing with LysoTracker staining in TLR2$^{-/-}$ BMDM.
D. Standardization of LysoTracker intensity by bacterial area among the population of *M. tuberculosis* H37Rv-infected or *M. tuberculosis* H37RvΔ*lppM*-infected TLR2$^{-/-}$ BMDM. All graphs are representative of at least two independent experiments.

implicated in cytokine production in a TLR2-independent manner, it appears that LppM displays its action through a mechanism different from that of other mycobacterial lipoproteins.

Discussion

In this study, we show that LppM limits *M. tuberculosis* uptake by macrophages and phagosomal maturation. ^{6}His-LppM$_{26–185}$ is able to complement the phenotype of *M. tuberculosis* H37RvΔ*lppM* with respect of phagocytosis, arguing for a direct involvement of LppM in macrophage uptake, regardless of LppM acylation. However, the addition of ^{6}His-LppM$_{26–185}$ to *M. tuberculosis* H37RvΔ*lppM* did not complement the phagosomal maturation phenotype, suggesting that the exogenous protein is not phagocytosed to the same extend as the live bacilli that is unstable once internalized by macrophage or that additional partners of LppM are required for its intracellular complementation. It has been previously reported that LprG, another

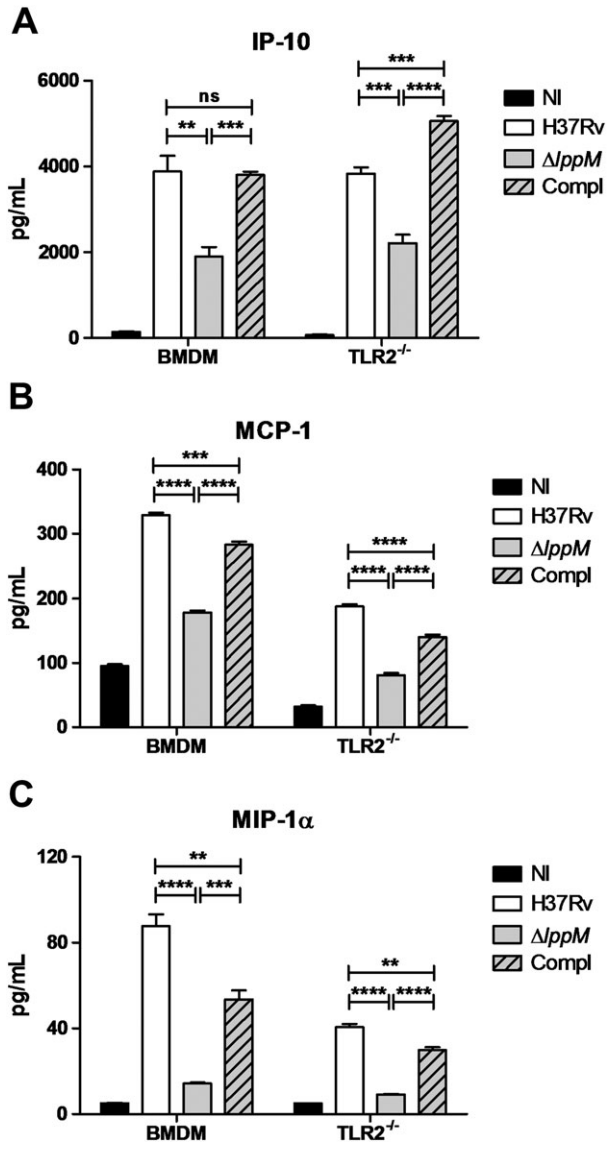

Fig. 5. *Mycobacterium tuberculosis* H37RvΔ*lppM* fails to fully induce the secretion of the pro-inflammatory chemokines. Secretion of (A) interferon-gamma-inducible protein-10 (IP-10), (B) monocyte chemoattractant protein-1 (MCP-1) and (C) macrophage inflammatory protein-1α (MIP-1α) in supernatant of non-infected (NI) and infected wild-type or toll-like receptor 2 (TLR2)$^{-/-}$ bone marrow-derived macrophages (BMDM) with *M. tuberculosis* H37Rv, *M. tuberculosis* H37RvΔ*lppM* or complemented strain (Compl).

mycobacterial lipoprotein, is able to control phagolysosomal fusion and that its action is mediated by the binding of LipoArabinoMannan (LAM) in its hydrophobic pocket (Gaur *et al.*, 2014; Shukla *et al.*, 2014), a lipoglycan known to be involved in this process. Therefore, it is tempting to hypothesize that the presence of ligands is required to fully complement the intracellular phenotype of *M. tuberculosis* H37RvΔ*lppM*, similarly to LprG with LAM. Consistent with this contention, we found that ^{6}His-LppM$_{26–185}$ produced by *Mycobacterium smegmatis* is able to bind PhosphatidylInositol Mannosides (PIM) derivatives, such as PI, PIM_2Ac_2 and PIM_6Ac_2 (Barthe *et al.*, unpublished), suggesting a role of these PIM derivatives in the LppM-mediated phagosomal maturation defect. Therefore, a defect in PIM presentation by *M. tuberculosis* H37RvΔ*lppM* could be directly responsible for the increased phagocytosis phenotype. Alternatively, the absence of LppM may have perturbed the general architecture of the mycobacterial cell wall and may have favoured the recognition of some other mycobacterial ligands by macrophages.

Several mycobacterial lipoproteins have been shown to be TLR2 agonists (Brightbill *et al.*, 1999; Gehring *et al.*, 2004; Pecora *et al.*, 2006; Drage *et al.*, 2009; Drage *et al.*, 2010; Lancioni *et al.*, 2011). Here, we show that LppM inhibits macrophage uptake of TB bacilli through a TLR2-dependent signalling, as *M. tuberculosis* H37Rv and *M. tuberculosis* H37RvΔ*lppM* show similar colocalization with acidified compartments within TLR2$^{-/-}$ BMDM. There is previous evidence that phagosomal maturation may be controlled by TLR-dependent signals, as *E. coli*-containing or *Staphylococcus aureus*-containing phagosomes can fuse with lysosomes in wild-type macrophages, whereas the phagosomes of MyD88$^{-/-}$ or TLR2x4$^{-/-}$ macrophages cannot (Blander and Medzhitov, 2004). TLR2 has also been shown to be expressed on the surface of phagosomes (Underhill *et al.*, 1999). Therefore, LppM would be able to trigger a TLR2 signalling while the bacilli reside in the extracellular environment and during its prolonged stay in the phagosomal compartment.

Mycobacterium tuberculosis H37RvΔ*lppM* induces lower levels of pro-inflammatory chemokines IP-10, MCP-1 and MIP-1α than *M. tuberculosis* H37Rv, reflecting a potential attenuation of the mutant on the very first hours of the infection. Indeed, IP-10 is expressed in very high amounts in patients with active TB and is one of the most promising alternative markers to interferon-gamma to detect patients with active TB (Ruhwald *et al.*, 2007). Furthermore, high levels of MCP-1 are correlated with the disease severity in TB patients (Hasan *et al.*, 2009). Moreover, infection of macrophages results in the induction of MIP-1α, which is required for the inhibition of *M. tuberculosis* growth (Saukkonen *et al.*, 2002). Interestingly, it was shown that non-capped lipoarabinomannan plays a direct role in inflammation by inducing the expression of MCP-1 and MIP-1α (Moller *et al.*, 2003). This could be in direct correlation with the binding of PIM derivatives by LppM in *M. smegmatis* mc^{2}155 (Barthe *et al.*, unpublished), considering that PIM are precursors of LAM. Consequently, for *M. tuberculosis* H37RvΔ*lppM*, a defect in the presentation of PIM derivatives by LppM or in the recognition of other mycobacterial ligands may potentially drive a decreased expression of both MCP-1 and MIP-1α.

It appears that mycobacterial lipoproteins display a large panel of cellular functions, ranging from phagosome–

lysosome fusion inhibition in the case of LprG to the induction of macrophage apoptosis in the case of LpqH (Sanchez *et al.*, 2012). Here, we propose that LppM is specialized in the initial steps of macrophage infection by *M. tuberculosis*. Increased macrophage uptake, impairment of the phagosomal maturation blocking and decreased pro-inflammatory chemokine production induced by *M. tuberculosis* H37RvΔ*lppM* are the hallmarks of a defect in efficient macrophage colonization, and these features highlight the importance of LppM for the initial steps of *M. tuberculosis* infection.

Experimental procedures

Bacterial strains

Escherichia coli TOP10 (Invitrogen) and *E. coli* BL21(DE3) (Stratagene) were used for cloning and expression of recombinant proteins (Table S1). All strains were grown in LB medium (Difco) at 37°C supplemented with ampicillin (100 $\mu g\,ml^{-1}$), hygromycin (100 $\mu g\,ml^{-1}$) or kanamycin (25 $\mu g\,ml^{-1}$), when required. *M. tuberculosis* H37Rv, *M. tuberculosis* H37RvΔ*lppM* and complemented strains were grown in Middlebrook 7H9 plus 0.05% Tween80 or on Middlebrook 7H11 agar plates, with OADC enrichment (Difco) supplemented with hygromycin (50 $\mu g\,ml^{-1}$) or kanamycin (25 $\mu g\,ml^{-1}$), when required. (Table S1).

Generation of a lppM *deletion mutant in* Mycobacterium tuberculosis *H37Rv*

To generate *M. tuberculosis* H37RvΔ*lppM*, we followed the protocol previously described by van Kessel *et al.* (van Kessel *et al.*, 2008). Briefly, upstream and downstream regions of *lppM* were amplified from *M. tuberculosis* H37Rv genomic DNA using [Up_*lppM*_dir and Up_*lppM*_rev] and [Down_*lppM*_dir and Down_*lppM*_rev] as primers (Table S2). Both fragments were inserted at either side of a hygromycin resistance cassette. After linearization, the resulting construction was electroporated in competent *M. tuberculosis* H37Rv containing pJV53 (Table S1) after acetamide induction. Several clones were selected and tested for the insertion of the hygromycin resistance cassette by PCR using Seq_*lppM*_dir and Seq_*lppM*_rev (Fig. S1A and Fig. S1B, Table S2). The resulting PCR fragment was further checked by sequencing to confirm the insertion at the expected *M. tuberculosis* locus. In addition, *M. tuberculosis* H37Rv and *M. tuberculosis* H37RvΔ*lppM* were transformed by pMRF1 (Table S1), a derivative of pMV261 carrying a kanamycin resistance cassette, which allows the expression of the red fluorescent protein DsRed.

Plasmid constructions

Fragments of *lppM* were amplified by PCR using *M. tuberculosis* H37Rv genomic DNA as a template and [pET15b_$lppM_{26\text{-}227}$_dir and pET15b_$lppM_{26\text{-}227}$_rev] or [pET15b_$lppM_{26\text{-}227}$_dir and pET15b_$lppM_{26\text{-}185}$_rev] (Table S2), containing NdeI and NheI sites, as primers. The resulting fragments were digested with NdeI and NheI and ligated into pETPhos, generating pETPhos::$lppM_{26\text{-}227}$ and pETPhos::$lppM_{26\text{-}185}$ (Table S1). The same approach was undertaken to insert *lppM* into pMV306 and pVV16, using the following pairs of primers [pMV306_*lppM*_dir and pMV306_*lppM*_rev] and [pVV16_*lppM*_dir and pVV16_*lppM*_rev] (Table S2), together with the relevant restriction enzymes, to obtain pMV306::$prom_{lppM}$::*lppM* and pVV16::*lppM* (Table S1). Finally, $prom_{hsp60}$::*lppM* was subcloned from pVV16::*lppM* into pMV306 using XbaI and ClaI to yield pMV306::$prom_{hsp60}$::*lppM* (Table S1). All plasmids were checked by sequencing.

Purification of recombinant ^{6}*His-LppM*

Escherichia coli BL21(DE3) strains containing pETPhos::$lppM_{26\text{-}227}$ or pETPhos::$lppM_{26\text{-}185}$ were used to inoculate 1 l of LB medium supplemented with ampicillin (100 $\mu g\,ml^{-1}$) and cultured at 37°C with shaking until the A_{600} reached ~0.5. Then, 1 mM (final concentration) of isopropyl 1-thio-β-d-galactopyranoside was added, and growth was continued for 3 h at 37°C. Soluble ^{6}His-$LppM_{26–227}$ and ^{6}His-$LppM_{26–185}$ were purified using Ni-NTA agarose beads (Qiagen) as previously described (Veyron-Churlet *et al.*, 2010).

Generation of anti-LppM antibodies and Western-blot analysis

Recombinant ^{6}His-$LppM_{26–227}$ purified from *E. coli* was used to generate specific rabbit antibodies against LppM according to the Speedy protocol (Eurogentec). Proteins were resolved by SDS-PAGE using 4–15% acrylamide gels (BioRad) and then transferred onto a polyvinylidene difluoride membrane. The membrane was saturated with TBS-Tween-5% milk and probed overnight with anti-LppM antibodies diluted 1:1000 with TBS-Tween-3% milk. The membrane was then incubated with anti-rabbit horseradish peroxidase-conjugated secondary antibodies (Jackson Immunoresearch) for 1 h at room temperature, followed by detection using Immobilon kit (Millipore). Chemiluminescence was determined using the ImageQuant LAS 4000 (GE Healthcare).

Cell culture

Wild-type and $TLR2^{-/-}$ bone marrow progenitors were obtained from tibias and femur bones of 7 to 11 week-old C57BL/6 mice and frozen at −80°C. The BMDM were obtained by seeding 10^{7} frozen bone marrow cells in 75 cm^{2} flasks in RPMI 1640 Glutamax medium (Gibco) supplemented with 10% heat-inactivated fetal bovine serum (FBS) (Gibco) and 10% L929-conditioned medium containing macrophage colony-stimulating factor. After 7 days of incubation at 37°C in 5% CO_2, BMDM were rinsed with Dulbecco's phosphate-buffered saline (D-PBS) and harvested with Versene (Gibco) for further use.

Mycobacterial preparation and labelling

Bacteria were harvested, washed three times and resuspended in PBS. The bacteria were allowed to stand for 30 min to allow residual aggregates to settle. The bacterial suspensions were then aliquoted and frozen at −80°C for further use. When needed, *M. tuberculosis* H37Rv, *M. tuberculosis* H37RvΔ*lppM* and the complemented strain ($prom_{lppM}$::*lppM*) were covalently labelled with CypHer5 mono ester

dye, which is a red-excitable cyanine dye derivative, available as an N-Hydroxysuccinimide ester that can be directly coupled to a broad range of cell surface receptors (Sigma Aldrich, Saint-Louis, MO). 10^8 bacteria were diluted in 300 μl of 0.1 mg ml^{-1} CypHer5E in 0.1 M sodium carbonate buffer (pH 9). The bacterial suspensions were incubated at 30°C under stirring at 600 r.p.m. and washed three times with PBS before use.

Infection for intracellular growth and LysoTracker assays

The bacteria were quantified by measuring the optical density (OD_{600}) and/or DsRed-fluorescence on a Victor Multilabel Counter (Perkin Elmer). The heat-killed bacteria were used as a positive control for infection in LysoTracker assays. Twenty microliter of bacterial suspensions and $LppM_{26\text{-}185}$-coated beads was seeded in 384-well plates (Greiner) at MOI ranging from 2 to 10 bacteria per cell. Then, 2.10^4 cells in a 30 μl volume were seeded per well. The plates were incubated at 37°C in 5% CO_2 for 2 h. To follow the mycobacterial replication in the BMDM, the cells were washed and treated for 1 h with 50 ng ml Amikacin (Sigma-Aldrich) to remove extracellular bacteria. Cells were finally incubated at 37°C with 5% CO_2 in complete culture medium containing a non-cytotoxic concentration of Hoechst (Sigma-Aldrich), corresponding to 300 ng ml^{-1}, to stain the cell nuclei. Image acquisition was performed daily. To study the phagosomal maturation/acidification, 50 μl of RPMI containing 1 μM of LysoTracker green DND-26 (Invitrogen) was added per well, and cells were incubated at 37°C with 5% CO_2 for 1.5 h. Cell nuclei were stained using 10 μg ml^{-1} Hoechst for 30 min at 37°C with 5% CO_2. Finally, cells were fixed with 10% neutral buffered Formalin solution (Sigma-Aldrich), containing paraformaldehyde at 4%, for 30 min at room temperature, washed in PBS and kept at 4°C in D-PBS 1% FBS until image acquisition.

Immunofluorescence assays

Macrophage infection was performed as described earlier. After 2 h of infection, cell monolayers were fixed with Formalin and permeabilized with D-PBS 0.2% Triton X100 for 5 min at room temperature. Cells were incubated for 30 min with blocking buffer, corresponding to 10% Donkey serum in D-PBS, prior to overnight incubation at 4°C with mouse anti-LAMP-1 [H4A3] (Abcam, Cambridge, UK) or goat anti-Cathepsin D (C-20) (Santa Cruz Biotechnology, Texas, USA) antibodies. Then, cells were incubated for 1 h at room temperature with Alexa-Fluor 488-conjugated goat anti-mouse and donkey anti-goat (Life technologies) secondary antibodies respectively. Cell nuclei were fluorescently labelled using 5 μg ml DAPI (Sigma-Aldrich) for 10 min. Cell monolayers were washed in PBS and kept in D-PBS 1% FBS until further use.

Image acquisition by automated confocal microscopy

Images were acquired using an automated fluorescent confocal microscope OPERA (PerkinElmer), with a 20X (Numeric Aperture 0.7) or 63X (NA 1.2) water immersion lens. The microscope was equipped with 405, 488, 561 and 640 nm excitation lasers. The emitted fluorescence was captured using three cameras associated with a set of filters covering a detection wavelength ranging from 450 to 690 nm. Nucleus staining with Hoechst was detected using the 405 nm laser (blue channel) with a 450/50 emission filter. LysoTracker-positive, LAMP-1-positive and cathepsin D-positive compartments (green channel) and mycobacteria (red channel) were detected on 488 and 561 nm laser with a 540/75 and 600/40 emission filters respectively. CypHer5E dye was detected with laser and filter that match the 644 nm absorbance and 663 nm emission wavelengths respectively.

Image-based analysis

For bacteria replication and acidic compartment colocalization, images were analysed using a multi-parameter script developed with Columbus system (version 2.3.1; PerkinElmer). Cells were detected and counted using internal methods provided by the software. The cell number and the bacterial area were determined by well. Intracellular bacterial growth was daily quantified by the ratio of bacterial area per cell divided by the bacterial area at Day 0. Acidic compartments stained by LysoTracker and bacteria were individually localized by a manual threshold method, using non-infected wells to determine the minimum threshold required to discard any background signals. The bacterial area was then stretched from 2 pixels to define the bacterial ring region. LysoTracker fluorescence area was detected in the red channel by keeping only pixels with a higher intensity than a manually defined threshold. Cells were split into four groups based on the presence (infected) or the absence (non-infected) of an intracellular bacterial signal and a LysoTracker positive or negative signal. Results are expressed as the average of all images in four different wells in at least three independent experiments. The percentage of infection and bacteria/LysoTracker colocalization was calculated as follows:

$$\%_{Population} = \frac{Nb\ \ of\ \ cells\ \ in\ \ the\ \ population}{Total\ \ Nb\ \ of\ \ cells} \times 100.$$

Lysosomal-associated membrane protein-1-positive and cathepsin D-positive compartments were identified according to an arbitrary threshold of fluorescence intensity, determined on non-infected cells, associated with anti-LAMP-1 or cathepsin D immunolabelling. The same thresholds were then applied to infected cells. The LAMP-1 and cathepsin D mean intensities were measured for each bacterium.

Infection for the determination of the cytokine profile

Murine macrophages were seeded at a density of 3.8×10^5 cells per well in 24-well plates. After 24 h, at 37°C in 5% CO_2, supernatants were removed, and cells were infected with 950 μl of *M. tuberculosis* H37Rv, *M. tuberculosis* H37RvΔ*lppM* or complemented strain ($prom_{lppM}$::*lppM*) suspensions to reach MOI of 1, 2 and 3. The plates were incubated at 37°C in 5% CO_2 for 5 or 24 h. The supernatants were then filtered using a 0.22 μM PVDF filter, sampled and stored at −80°C until analysis. Mouse cytokine concentrations were quantified using Cytokine Mouse Magnetic 20-Plex Panel kit (Life Technologies) and Luminex® platform, accordingly to the manufacturer's protocol.

Statistics

For bacteria replication and acidic compartment colocalization using the LysoTracker probe, the statistical significance (*P*-value) was tested with a two-tailed unpaired *t*-test (GraphPad Prism version 5.04), and *P*-values ≤ 0.05 were considered to show significant differences. For the comparison of the LAMP-1 and cathepsin D mean intensities obtained for wild-type and mutant bacteria, the statistical significant value was obtained using a Wilcoxon unpaired test (or Mann–Whitney *U*-test).

Acknowledgements

We thank Dr Sang Hyun Cho (Institute for Tuberculosis Research, Chicago, USA) for kindly providing pMRF1. RVC acknowledges support from the Région Nord-Pas-de-Calais. Financial support for this work was provided by the European Community (ERC-STG INTRACELLTB Grant no 260901, MM4TB Grant no 260872), the Agence Nationale de la Recherche (ANR-10-EQPX-04-01, ANR-14-CE14-0024-03), the Projet Transversal de Recherche de l'Institut Pasteur (PTR441), the Feder (12001407 (D-AL) Equipex Imaginex BioMed) and the Région Nord-Pas-de-Calais (convention no 12000080).

References

Barry, C.E., 3rd, Boshoff, H.I., Dartois, V., Dick, T., Ehrt, S., Flynn, J., *et al.* (2009) The spectrum of latent tuberculosis: rethinking the biology and intervention strategies. *Nat Rev Microbiol* **7**: 845–855.

Blander, J.M., and Medzhitov, R. (2004) Regulation of phagosome maturation by signals from toll-like receptors. *Science* **304**: 1014–1018.

Brightbill, H.D., Libraty, D.H., Krutzik, S.R., Yang, R.B., Belisle, J.T., Bleharski, J.R., *et al.* (1999) Host defense mechanisms triggered by microbial lipoproteins through toll-like receptors. *Science* **285**: 732–736.

Brodin, P., Majlessi, L., Marsollier, L., de Jonge, M.I., Bottai, D., Demangel, C., *et al.* (2006) Dissection of ESAT-6 system 1 of *Mycobacterium tuberculosis* and impact on immunogenicity and virulence. *Infect Immun* **74**: 88–98.

Brodin, P., Poquet, Y., Levillain, F., Peguillet, I., Larrouy-Maumus, G., Gilleron, M., *et al.* (2010) High content phenotypic cell-based visual screen identifies *Mycobacterium tuberculosis* acyltrehalose-containing glycolipids involved in phagosome remodeling. *PLoS Pathog*: 6.

Cambier, C.J., Takaki, K.K., Larson, R.P., Hernandez, R.E., Tobin, D.M., Urdahl, K.B., *et al.* (2014) Mycobacteria manipulate macrophage recruitment through coordinated use of membrane lipids. *Nature* **505**: 218–222.

Drage, M.G., Pecora, N.D., Hise, A.G., Febbraio, M., Silverstein, R.L., Golenbock, D.T., *et al.* (2009) TLR2 and its co-receptors determine responses of macrophages and dendritic cells to lipoproteins of *Mycobacterium tuberculosis*. *Cell Immunol* **258**: 29–37.

Drage, M.G., Tsai, H.C., Pecora, N.D., Cheng, T.Y., Arida, A.R., Shukla, S., *et al.* (2010) *Mycobacterium tuberculosis* lipoprotein LprG (Rv1411c) binds triacylated glycolipid agonists of Toll-like receptor 2. *Nat Struct Mol Biol* **17**: 1088–1095.

Dubnau, E., Fontan, P., Manganelli, R., Soares-Appel, S., and Smith, I. (2002) *Mycobacterium tuberculosis* genes induced during infection of human macrophages. *Infect Immun* **70**: 2787–2795.

Gaur, R.L., Ren, K., Blumenthal, A., Bhamidi, S., Gibbs, S., Jackson, M., *et al.* (2014) LprG-mediated surface expression of lipoarabinomannan is essential for virulence of *Mycobacterium tuberculosis*. *PLoS Pathog* **10** e1004376.

Gehring, A.J., Dobos, K.M., Belisle, J.T., Harding, C.V., and Boom, W.H. (2004) *Mycobacterium tuberculosis* LprG (Rv1411c): a novel TLR-2 ligand that inhibits human macrophage class II MHC antigen processing. *J Immunol* **173**: 2660–2668.

Harding, C.V., and Boom, W.H. (2010) Regulation of antigen presentation by *Mycobacterium tuberculosis*: a role for Toll-like receptors. *Nat Rev Microbiol* **8**: 296–307.

Hasan, Z., Cliff, J.M., Dockrell, H.M., Jamil, B., Irfan, M., Ashraf, M., and Hussain, R. (2009) CCL2 responses to *Mycobacterium tuberculosis* are associated with disease severity in tuberculosis. *PLoS One* **4** e8459.

Killick, K.E., Ni Cheallaigh, C., O'Farrelly, C., Hokamp, K., MacHugh, D.E., and Harris, J. (2013) Receptor-mediated recognition of mycobacterial pathogens. *Cell Microbiol* **15**: 1484–1495.

Klopper, M., Warren, R.M., Hayes, C., Gey van Pittius, N.C., Streicher, E.M., Muller, B., *et al.* (2013) Emergence and spread of extensively and totally drug-resistant tuberculosis, South Africa. *Emerg Infect Dis* **19**: 449–455.

Lancioni, C.L., Li, Q., Thomas, J.J., Ding, X., Thiel, B., Drage, M.G., *et al.* (2011) *Mycobacterium tuberculosis* lipoproteins directly regulate human memory CD4(+) T cell activation via Toll-like receptors 1 and 2. *Infect Immun* **79**: 663–673.

Li, W., Fan, X., Long, Q., Xie, L., and Xie, J. (2015) *Mycobacterium tuberculosis* effectors involved in host-pathogen interaction revealed by a multiple scales integrative pipeline. In *Infection, genetics and evolution : journal of molecular epidemiology and evolutionary genetics in infectious diseases*, Vol. **32**, pp. 1–11.

Moller, A.S., Ovstebo, R., Westvik, A.B., Joo, G.B., Haug, K.B., and Kierulf, P. (2003) Effects of bacterial cell wall components (PAMPs) on the expression of monocyte chemoattractant protein-1 (MCP-1), macrophage inflammatory protein-1alpha (MIP-1alpha) and the chemokine receptor CCR2 by purified human blood monocytes. *J Endotoxin Res* **9**: 349–360.

Pecora, N.D., Gehring, A.J., Canaday, D.H., Boom, W.H., and Harding, C.V. (2006) *Mycobacterium tuberculosis* LprA is a lipoprotein agonist of TLR2 that regulates innate immunity and APC function. *J Immunol* **177**: 422–429.

Ruhwald, M., Bjerregaard-Andersen, M., Rabna, P., Kofoed, K., Eugen-Olsen, J., and Ravn, P. (2007) CXCL10/IP-10 release is induced by incubation of whole blood from tuberculosis patients with ESAT-6, CFP10 and TB7.7. In *Microbes and infection/Institut Pasteur*, Vol. **9**, pp. 806–812.

Sanchez, A., Espinosa, P., Garcia, T., and Mancilla, R. (2012) The 19 kDa *Mycobacterium tuberculosis* lipoprotein (LpqH) induces macrophage apoptosis through extrinsic and intrinsic pathways: a role for the mitochondrial apoptosis-inducing factor. *Clin Dev Immunol* **2012**: 950503.

Saukkonen, J.J., Bazydlo, B., Thomas, M., Strieter, R.M., Keane, J., and Kornfeld, H. (2002) Beta-chemokines are induced by *Mycobacterium tuberculosis* and inhibit its growth. *Infect Immun* **70**: 1684–1693.

Shukla, S., Richardson, E.T., Athman, J.J., Shi, L., Wearsch, P. A., McDonald, D., *et al.* (2014) *Mycobacterium tuberculosis* lipoprotein LprG binds lipoarabinomannan and determines its cell envelope localization to control phagolysosomal fusion. *PLoS Pathog* **10** e1004471.

Stanley, S.A., and Cox, J.S. (2013) Host–pathogen interactions during *Mycobacterium tuberculosis* infections. *Curr Top Microbiol Immunol* **374**: 211–241.

Underhill, D.M., Ozinsky, A., Smith, K.D., and Aderem, A. (1999) Toll-like receptor-2 mediates mycobacteria-induced proinflammatory signaling in macrophages. *Proc Natl Acad Sci U S A* **96**: 14459–14463.

van Kessel, J.C., Marinelli, L.J., and Hatfull, G.F. (2008) Recombineering mycobacteria and their phages. *Nat Rev Microbiol* **6**: 851–857.

Vergne, I., Chua, J., Lee, H.H., Lucas, M., Belisle, J., and Deretic, V. (2005) Mechanism of phagolysosome biogenesis block by viable *Mycobacterium tuberculosis*. *Proc Natl Acad Sci U S A* **102**: 4033–4038.

Veyron-Churlet, R., Zanella-Cleon, I., Cohen-Gonsaud, M., Molle, V., and Kremer, L. (2010) Phosphorylation of the *Mycobacterium tuberculosis* beta-ketoacyl-acyl carrier protein reductase MabA regulates mycolic acid biosynthesis. *J Biol Chem* **285**: 12714–12725.

Walburger, A., Koul, A., Ferrari, G., Nguyen, L., Prescianotto-Baschong, C., Huygen, K., *et al.* (2004) Protein kinase G from pathogenic mycobacteria promotes survival within macrophages. *Science* **304**: 1800–1804.

Young, D.B., Gideon, H.P., and Wilkinson, R.J. (2009) Eliminating latent tuberculosis. *Trends Microbiol* **17**: 183–188.

Supporting information

Additional supporting information may be found in the online version of this article at the publisher's web-site:

Fig. S1. Generation of *M. tuberculosis* H37RvΔ*lppM*. (A) Genomic organization of the *lppM* locus in *M. tuberculosis* H37Rv and schematic representation of the insertion of the hygromycin cassette resistance. Primers 1 and 2 used for PCR are symbolized by arrows. (B) PCR using primers 1 and 2 with genomic DNA extracted from *M. tuberculosis* H37Rv or *M. tuberculosis* H37RvΔ*lppM*. (C) Western-blot analysis on crude lysates of *M. tuberculosis* H37Rv and *M. tuberculosis* H37RvΔ*lppM* cultures using polyclonal antibodies against LppM and anti-Hsp65 monoclonal antibodies, used as a control. (D) Western-blot analysis using anti-LppM antibodies on crude lysates of *M. tuberculosis* H37RvΔ*lppM* transformed by integrative empty vector (pMV306), vector containing *lppM* under the control of its own promoter ($prom_{lppM}$::*lppM*), vector containing *lppM* under the control of the strong *hsp60* promoter ($prom_{hsp60}$::*lppM*) and the recombinant mature ^{6}His-Lpp$M_{26\text{-}227}$ purified from *E. coli*.

Fig. S2. Analysis of *M. tuberculosis* H37RvΔ*lppM* phenotype after infection of BMDM. (A) Median of the bacterial area after infection of BMDM by *M. tuberculosis* H37Rv, *M. tuberculosis* H37RvΔ*lppM* or respective heat-killed bacteria (MOI 10) as a control. (B) Fold change of the bacterial area after infection of BMDM by *M. tuberculosis* H37Rv or *M. tuberculosis* H37RvΔ*lppM* (using a MOI of 2) from Day 0 to Day 4. (C) Percentage of Lysotracker-positive BMDM 2 h post-infection, using *M. tuberculosis* H37Rv, *M. tuberculosis* H37RvΔ*lppM* or the complemented strain ($prom_{lppM}$::*lppM*) labelled with CypHer5E.

Table S1. List of strains and plasmids used in this study.

Table S2. List of primers used in this study.

